ADMET & DMPK 13(3) (2025) 2733; doi: https://doi.org/10.5599/admet.2733

ADMET

Open Access : ISSN : 1848-7718

http://www.pub.iapchem.org/ojs/index.php/admet/index

Original scientific paper

Epirubicin-sensitive detection with a $CoWO_4$/reduced graphene oxide modified screen-printed electrode

Somayeh Tajik[1,*], Razieh Moghimian[1] and Hadi Beitollahi[2]

[1]*Research Centre of Tropical and Infectious Diseases, Kerman University of Medical Sciences, Kerman, Iran*
[2]*Environment Department, Institute of Science and High Technology and Environmental Sciences, Graduate University of Advanced Technology, Kerman, Iran*

Corresponding Author: E-mail: *tajik_s1365@yahoo.com*

Received: February 26, 2025; Revised: April 22, 2025; Published: May 8, 2025

Abstract

Background and purpose: Because of its antimetabolic and cytotoxic qualities, epirubicin (EP), a crucial chemotherapeutic drug, has been used to treat a number of cancers, including those of the prostate, breast, ovary, stomach, lung, and colon. **Experimental approach:** In this study, $CoWO_4$/reduced graphene oxide ($CoWO_4$/rGO) nanocomposite was synthesised and characterised by field emission-scanning electron microscopy and energy-dispersive X-ray spectroscopy. To provide a novel sensing platform for EP determination, a screen-printed electrode (SPE) surface was modified using the as-fabricated $CoWO_4$/rGO nanocomposite. **Key results:** Using voltammetric techniques, the electrochemical behaviour of the $CoWO_4$/rGO nanocomposite modified SPE ($CoWO_4$/rGO/SPE) for the EP detection was examined. $CoWO_4$/rGO significantly reduced the overpotential of the EP redox reaction and increased the rate of electron transfer between the electrode and analyte as compared to bare SPE. EP was quantitatively analysed using differential pulse voltammetry. **Conclusions:** It was discovered that the linearity range was 0.01 to 190.0 μM. The sensitivity and limit of detection were 0.1529 μA μM^{-1} and 0.007 μM, respectively. Additionally, the constructed $CoWO_4$/rGO/SPE sensor's practical applicability was investigated in pharmaceutical samples with good recovery outcomes.

Keywords

$CoWO_4$/reduced graphene oxide nanocomposite; chemically modified electrode, urine sample, cancer, drug analysis

Introduction

One of the anthracycline derivatives is epirubicin (EP). Because of its cytotoxic and antimetabolic qualities, EP has been used as a key chemotherapeutic drug to treat breast, prostate, ovarian, gastric, lung, and colorectal cancers, among other cancers. In patients with prostate cancer, EP has continuously shown cytotoxic effects, whether given as a monotherapy or in combination with other treatment drugs [1-5]. It is still unclear exactly what method EP works via. It has been suggested that the chemical mainly targets the fast DNA replication in cancerous cells. The steric changes that are incorporated into the structure of EP affect the stability of the DNA-anthracycline complex, which causes the analogue to enter and exit the tumour and normal cells more quickly (which breaks the helical structure of DNA), which in turn prevents the synthesis and replication of DNA and RNA and tumour cell growth [6-11]. The evaluation of EP concentrations in human biological fluids is helpful in adjusting pharmacological dosages in the treatment strategy that targets cancer cells because of the potentially

dangerous nature of high medication dosages for patients. The measurement of EP in genuine samples has been accomplished using a variety of approaches and quantitative analytical techniques, such as spectrophotometric techniques, electrophoresis, and liquid chromatography (LC) [12-19]. Trace quantities of EP in pharmaceutical formulations and biological specimens have been widely detected using electrochemical techniques, which are known for their ease of use, sensitivity, and affordability [20-22].

With its small shape and ability to link to portable equipment for on-site analyte detection, screen-printed electrodes (SPEs) made using microfabrication technology have three electrodes printed on a single strip. These devices may also be surface-modified with different compositions and have a versatile design. SPEs support green chemical concepts, such as the creation of safe products, and are affordable, simple to manufacture, and appropriate for mass production. Furthermore, SPEs provide great sensitivity, low energy consumption, linear response, and the ability to operate efficiently at room temperature [23-26].

Unmodified electrodes often have low sensitivity and a high over-potential, which causes surface fouling to build up gradually over time. The electrode surface must be modified for the electrochemical detection of different analytes. Enhancing the electron exchange between the electrode surface and the electro-active species is the primary objective of electrode modification. Consequently, several investigations have been carried out to create modified electrodes utilizing a range of substances and nanostructures [27-32]. High specific surface area, exceptional conductivity, a large number of surface-active sites, and potent catalytic activity are some benefits of nanomaterials. These features can significantly increase the stability and sensitivity of sensors. Additionally, nanomaterials can facilitate electrochemical processes and improve electron transfer efficiency by acting as catalysts. Carbon nanostructures have many structural and property differences, including graphene oxide (GO) and its derivatives, which lead to various uses. Since its discovery, graphene, one of the carbon allotropes, has made tremendous strides in studying carbon nanostructures. A two-dimensional honeycomb lattice of carbon atoms is used to form single-layer graphene sheets. GO's huge surface area and electrical conductivity, among other qualities, make it a perfect and valuable material for various electrochemical applications, such as energy conversion, sensing, and storage [33-37].

Because of the synergistic effects between two transition metals, binary transition metal oxides (BTMOs) have outstanding electrochemical characteristics, making them effective and appropriate electrode materials. $CoWO_4$ stands out as a noteworthy molecule with potent chemical and catalytic capabilities. Many attempts have been made to improve BTMOs' electrochemical performance. One efficient strategy is developing a technique for combining highly conductive carbon nanostructures with binary transition metal oxides to create a nanocomposite [37-45]. Because of their high electrical conductivity, large surface area, and advantageous mechanical properties, carbon nanostructures, like two-dimensional reduced graphene oxide (rGO), can be integrated with BTMOs to greatly enhance the electrical conductivity and electrochemical properties of the resulting nanocomposites [46,47].

Using a $CoWO_4$/rGO nanocomposite, this work offers a simple and sensitive electrochemical sensing platform for improved EP detection. Due to its greater electrical conductivity and bigger active surface area, the $CoWO_4$/rGO/SPE sensing platform demonstrated better electrochemical performance for EP detection than unmodified SPE. With a low limit of detection (LOD) and good sensitivity over a broad linear detection range, quantitative studies showed that the proposed sensor had exceptional electrochemical sensing capabilities for EP determination. Additionally, examining the injection sample showed how well the developed sensor worked. This work's main novelty is the effective modification of SPE in the voltammetric determination of EP using the $CoWO_4$/rGO nanocomposite, which has beneficial features.

Experimental

Apparatus and chemicals

Electrochemical measurements are conducted using an Autolab potentiostat/galvanostat. A screen-printed electrode (SPE) from DropSens (DRP-110, Spain) is utilized, incorporating three standard electrodes: a silver pseudo-reference electrode, a graphite counter electrode, and a graphite working electrode. pH measurements are performed using a Metrohm 710 pH meter. All other reagents, including epirubicin, were of analytical grade and sourced from Merck. Buffer solutions were prepared with orthophosphoric acid and its corresponding salts, covering a pH range of 2.0 to 9.0.

Synthesis of $CoWO_4$/rGO nanocomposite

With a few adjustments, the $CoWO_4$/rGO nanocomposite's synthesis was carried out using the methodology described by Xu *et al*. [48]. To do this, 60 mg of GO was dissolved in 40 mL of deionised water, and the mixture was ultrasonically agitated for one hour to create an aqueous suspension of GO. Following ultrasonication, the aforementioned suspension was mixed with aqueous solutions (10 mL containing 2 mmol $CoCl_2 \cdot 6H_2O$ (0.475 g) and 10 mL containing 2 mmol $Na_2WO_4.2H_2O$ (0.659 g)) and magnetically swirled for one hour. The GO suspension with metal salts was then put into a 100 mL stainless-steel autoclave lined with Teflon. It was then baked for 12 hours at 180 °C before cooling naturally to room temperature. The product, which was produced after washing and drying at 70 °C for 15 hours, was identified as the $CoWO_4$/rGO nanocomposite after the prepared precipitate was collected by centrifugation. Figure 1 shows an atypical FE-SEM.

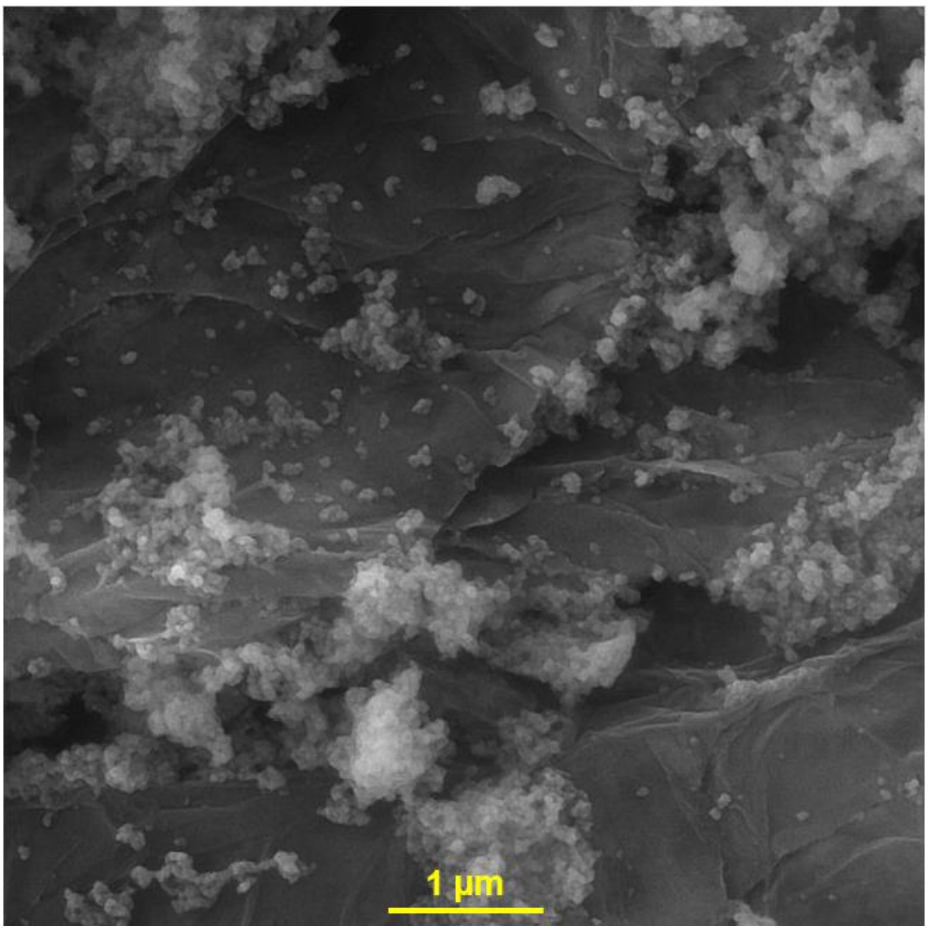

Figure 1. FE-SEM image of $CoWO_4$/rGO nanocomposite

Additionally, the EDX analysis (Figure 2) shows that the prepared nanocomposite contains Co, W, C, and O elements without any impurities.

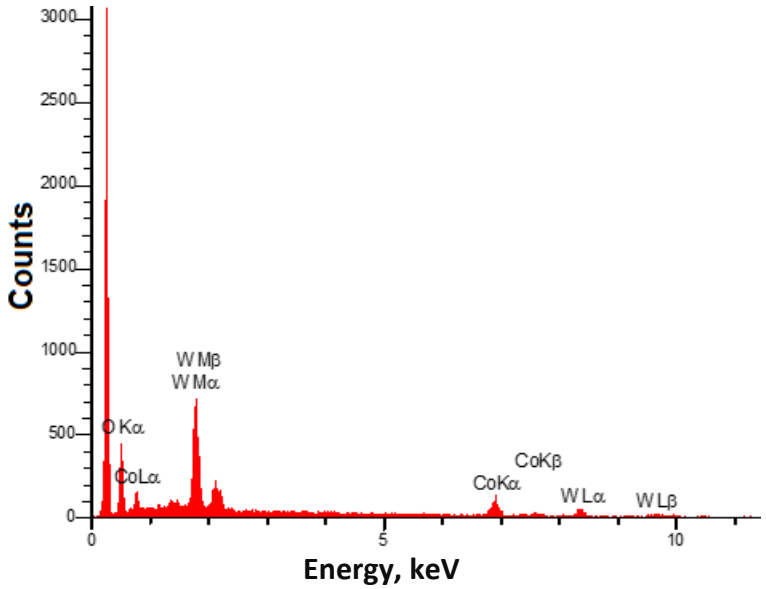

Figure 2. EDX spectrum of $CoWO_4$/rGO nanocomposite

Preparation of the electrode

A CoWO4/rGO nanocomposite is added to the screen-printed working electrode using a straightforward drop-casting technique. After 30 minutes of ultrasonication, the $CoWO_4$/reduced graphene oxide nanocomposite (1 mg) was dispersed in 1 millilitre of the aqueous solution to create the stock solution. The screen-printed working electrode surface is then covered with a 5 µl CoWO4/rGO nanocomposite suspension. After that, the solvent was allowed to evaporate at room temperature.

Preparation of real samples

Immediately after collection, the drug-free human urine specimens are kept in a refrigerator. First, 10 ml of each sample was utilised and centrifuged for 600 s at 2000 rpm. A 0.45 µm filter was used to filter the supernatant. After that, different amounts of the treated urine samples were collected, put in a flask, and diluted using a pH 7.0 phosphate buffer solution (PBS). Different amounts of epirubicin were added to these samples. The concentrations of epirubicin are measured using the standard addition method.

10.0 mL of PBS (0.1 M) at pH 7.0 was combined with 1.0 mL of an epirubicin ampoule that contained 2 mg in 1 mL. To attain the calibration mark, various amounts of the resultant diluted solution were poured into a series of 25 mL volumetric flasks and further diluted with PBS solution. The standard addition method was used to conduct the study.

Results and discussion

Electrochemical behaviour of EP on the various electrodes

In the pH range of 2.0 to 9.0, the effect of pH on the present responsiveness of $CoWO_4$/rGO/SPE towards EP oxidation was investigated. The findings showed that at a pH of 7.0, the current response of $CoWO_4$/rGO/SPE to EP oxidation peaked. Therefore, pH 7.0 was chosen for more research and analysis. To assess the $CoWO_4$/rGO nanocomposite's performance in the electrochemical measurement of EP, cyclic voltammetry tests was conducted (Figure 3). The CV responses of the $CoWO_4$/rGO/SPE (curve b) and an unmodified SPE (curve a) were measured in 0.1 M PBS at pH 7.0 with 100.0 µM EP. As can be observed, both the modified and unmodified electrodes displayed distinct anodic/cathodic redox peaks for EP. On the $CoWO_4$/rGO/SPE, however, a significant impact on EP detection was noted. For the redox reaction of EP, the unmodified SPE showed a poor voltammetric response, resulting in comparatively lower current values.

Compared to bare electrodes, the $CoWO_4$/rGO/SPE showed a stronger voltammetric response to EP. Furthermore, in contrast to the unmodified SPE, the redox peaks of EP were observed at lower potentials in the $CoWO_4$/rGO/SPE. The beneficial benefits of the $CoWO_4$/rGO nanocomposite and their synergistic effects may be the reason for the $CoWO_4$/rGO/SPE's higher sensitivity to EP as compared to bare SPE, according to the comparison of these CVs.

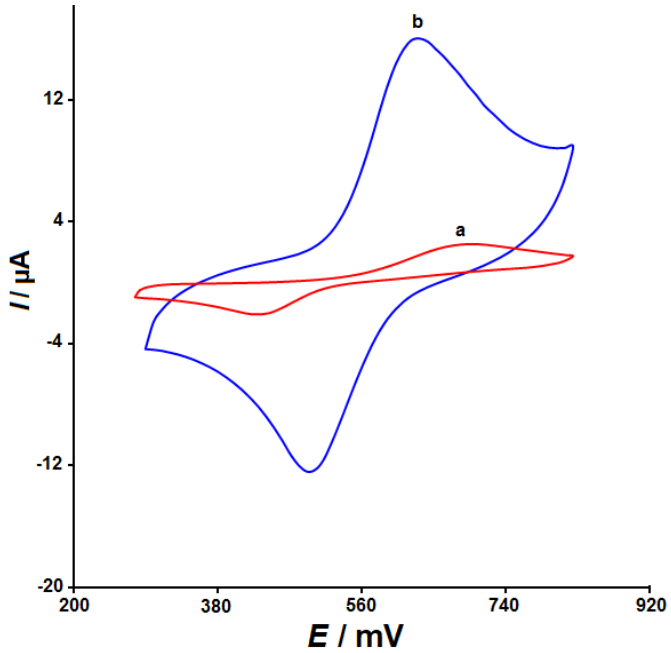

Figure 3. The cyclic voltammograms of (a) bare SPE and (b) $CoWO_4$/rGO/SPE at a scan rate of 50 mVs^{-1} with 100.0 µM epirubicin in 0.1 M PBS at pH 7

Effect of scan rate

To examine the impact of scan rates between 10 and 400 mV s^{-1} on the redox peak currents (I_{pa}, I_{pc}) and peak potential, CVs of 100.0 µM EP were recorded using the $CoWO_4$/rGO/SPE sensor at varying scan rates (Figure 4).

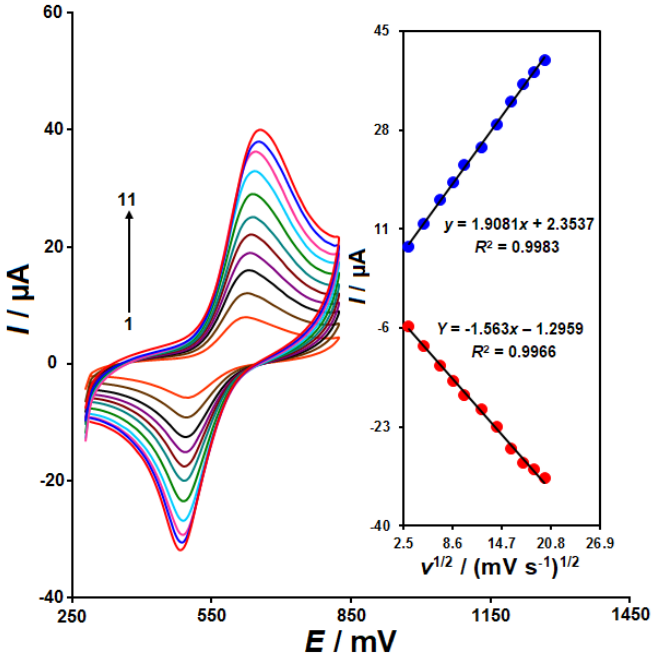

Figure 4. Cyclic voltammograms of 100.0 µM EP at the $CoWO_4$/rGO/SPE surface in 0.1 M PBS (pH 7.0) at various scan rates (1-11 respectively, corresponding to 10, 25, 50, 75, 100, 150, 200, 250, 300, 350 and 400 mV s^{-1}). Inset: redox peak currents plotted linearly against $v^{1/2}$

As the scan rate increases, the peak current magnitude rises accordingly. Simultaneously, the oxidation peak potential of EP shifts toward more positive values, while the reduction peak potential moves toward more negative values. The inset of Figure 4 shows a linear relationship between redox peak currents and the square root of the scan rate ($\nu^{1/2}$) for EP. This result demonstrates that the $CoWO_4$/rGO/SPE surface is diffusion-controlled for the redox process of EP.

Chronoamperometric studies

The chronoamperometric evaluations of different EP concentrations performed at the $CoWO_4$/rGO/SPE are shown in Figure 5. This method makes it possible to calculate the diffusion coefficient (*D)* of EP. For an electro-active species with a diffusion coefficient (D / cm^2 s^{-1}), the current of an electrochemical reaction is described by the Cottrell equation ($I = nFAC_bD^{1/2}\pi^{-1/2}t^{-1/2}$). The best-fit curves were used for the different EP levels (Inset A (Figure 5). The slope of the derived linear equations was then displayed against the EP levels (Inset B, Figure 4). The *D* parameter for EP was determined to be 1.5×10^{-5} cm^2 s^{-1} using the Cottrell equation to the slopes found in the experimental plots.

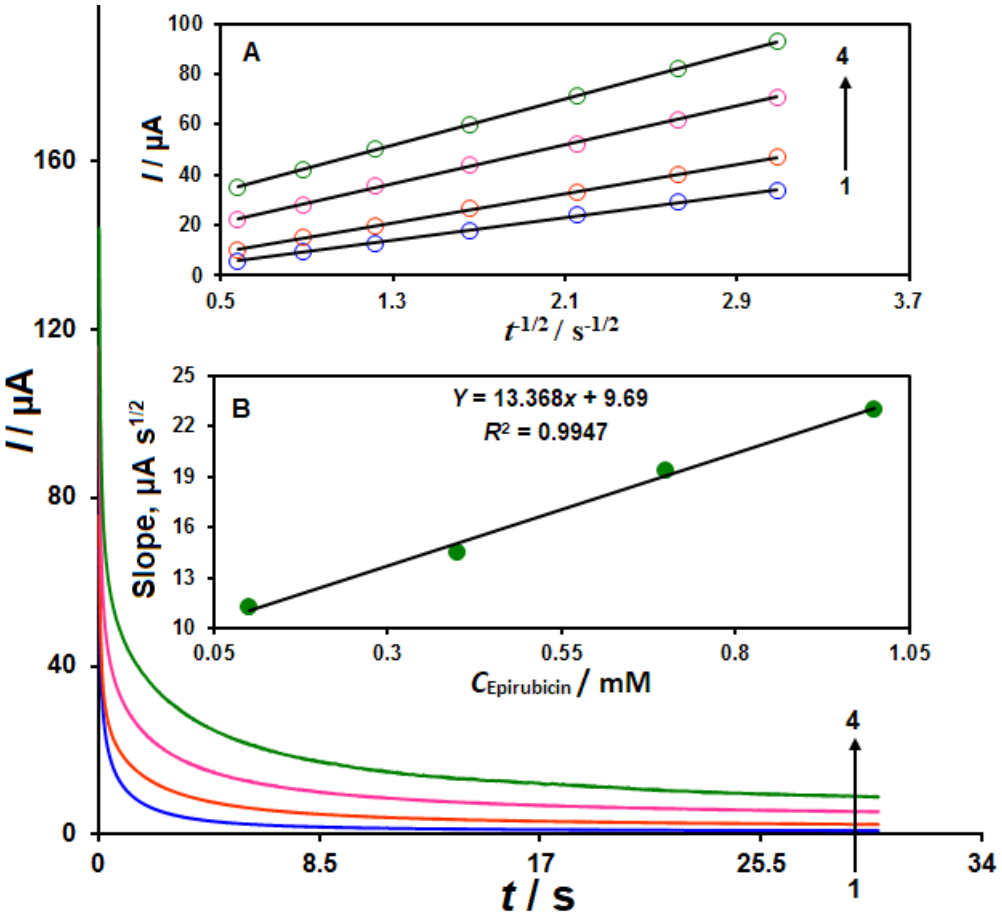

Figure 5. Chronoamperograms of EP at different concentrations (0.1 to 1.0 mM) acquired at $CoWO_4$/rGO/SPE in PBS (0.1 M with pH 7.0). The concentrations of EP represented by the numbers 1 to 4 are 0.1, 0.4, 0.7 and 1.0 mM. *I* vs. $t^{-1/2}$ linear graphs obtained from chronoamprograms are shown in Inset A, and the slopes of these lines are shown against C_{EP} in Inset B

Voltammetric detection of EP on $CoWO_4$/rGO/SPE

The main goal of this analysis is to develop a sensing electrode for the detection of low EP concentrations using a $CoWO_4$/rGO nanocomposite. Thus, DPV was used to study the oxidation of EP at $CoWO_4$/rGO/SPE in 0.1 M PBS (pH 7.0) by adjusting its concentration between 0.01 and 190.0 µM under the ideal circumstances of 50 mV s^{-1} scan rate, 0.01 V step potential, and 0.025 V pulse amplitude (Figure 6). A plot of I_{pa} against EP concentration is shown in Figure 6 (Inset), which shows a linear connection between I_{pa} and EP concentration.

As the concentration of EP rises, so does the peak current. The linearity is obtained in the range of 0.01 and 190.0 µM. Additionally, 0.007 µM was determined to be the LOD value.

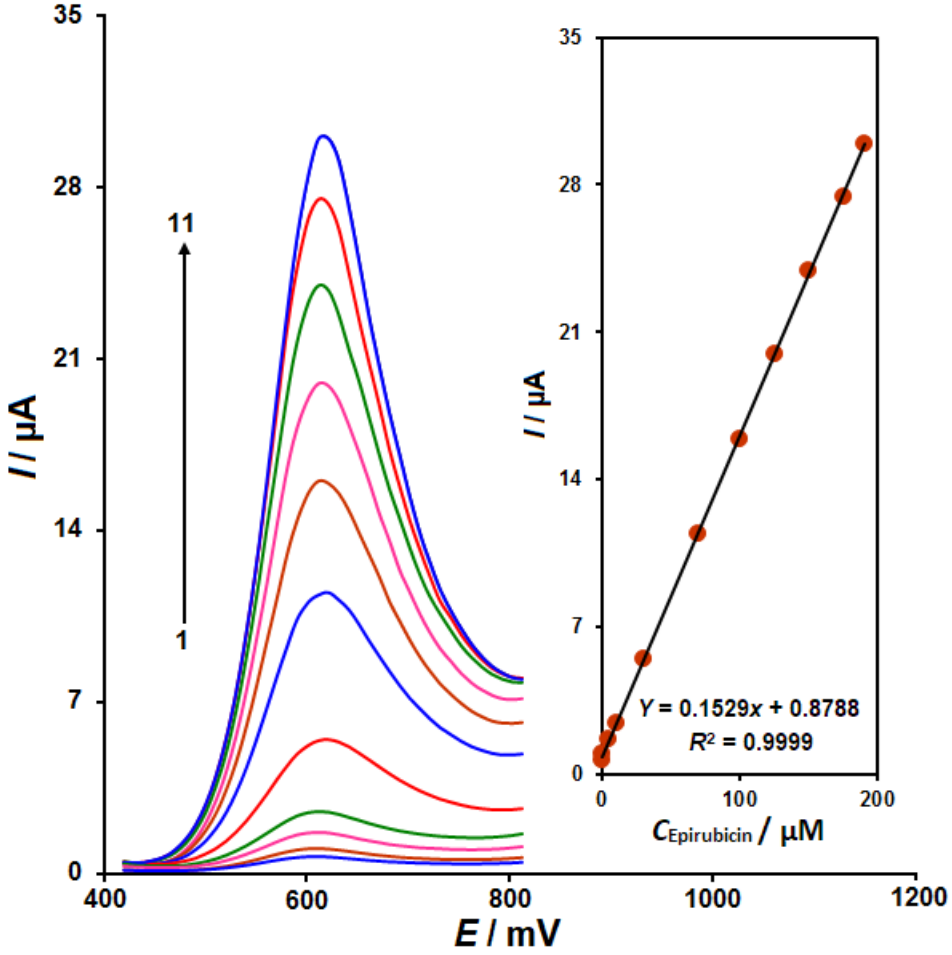

Figure 6. The recorded DPVs for the $CoWO_4$/rGO/SPE in the 0.1 M PBS at pH 7.0 containing EP at different concentrations (voltammograms 1 to 11 related to 0.01, 0.1, 5.0, 10.0, 30.0, 70.0, 100.0, 125.0, 150.0, 175.0 and 190.0 µM, respectively). Inset: Corresponding calibration plot of I_{pa} *vs.* concentrations of EP

Repeatability and selectivity studies

The DPV responses at $CoWO_4$/rGO/SPE in PBS 0.1 M (pH 7.0) towards 70.0 µM EP were recorded 15 times to determine the devised approach's repeatability. The modified SPE preserved 98.8 % of its current response from the initial test, indicating strong repeatability, according to measurements conducted under identical circumstances.

The DPV measurements were carried out in 0.1 M PBS with 70.0 µM EP in the presence of several interferents to evaluate the selectivity of the $CoWO_4$/rGO/SPE sensor. The results revealed that the current response of EP was not significantly affected by glucose, dopamine, L-cysteine, glycine, and tryptophan, Na^+, K^+, Br^- and NO_3^- (the signal change was less than ±5 %).

Practical application $CoWO_4$/rGO/SPE sensor in real specimens

The $CoWO_4$/rGO/SPE was utilised to assess EP in urine samples and injection using the standard addition method to demonstrate the created sensor's applicability. The findings of this study are displayed in Table 1. The results showed that recoveries that ranged from 97.3 to 104.4 % were satisfactory. Furthermore, the designed sensor's excellent accuracy was demonstrated by the obtained RSDs (n = 5) being less than 3.6%. Thus, it is possible to analyse EP in actual specimens using the $CoWO_4$/rGO/SPE sensor.

Table 1. Utilizing the $CoWO_4$/rGO/SPE sensor to measure EP in actual samples

Sample	Added concentration, µM	Found concentration, µM	Recovery, %	RSD, %
EP injection	0	4.1	-	3.4
	1.0	5.0	98.0	2.1
	3.0	7.3	102.8	1.8
	5.0	9.5	104.4	2.9
	7.0	11.0	99.1	3.0
Urine	0	-	-	-
	5.0	5.1	102.0	1.8
	7.5	7.3	97.3	3.6
	10.0	10.4	104.0	2.2
	12.5	12.4	99.2	2.7

Conclusion

The $CoWO_4$/rGO nanocomposite was created using a straightforward process and examined using the FE-SEM and EDX methods. EP was determined voltammetrically using $CoWO_4$/rGO/SPE. Excellent EP detection capabilities are demonstrated by the $CoWO_4$/rGO/SPE due to the synergy between $CoWO_4$ and rGO. With a low limit of detection of 0.007 µM, the developed sensor displayed linear dynamic ranges in the range of 0.01-190.0 µM of EP concentration. To sum up, the suggested sensor has been shown to be a reliable instrument for precisely detecting EP in actual specimens, producing positive outcomes.

***Acknowledgements**: This study was financially supported by the Research Centre of Tropical and Infectious Diseases, Kerman University of Medical Sciences, Kerman, Iran (grant number 403000792 and research ethics committees code of IR.KMU.REC.1403.437).*

***Declaration of competing interest:** The authors have no declaration of interest.*

***Data availability statement:** The data presented in this study are available on request from the corresponding authors.*

References

[1] A.B. Hashkavayi, J.B. Raoof. Design an aptasensor based on structure-switching aptamer on dendritic gold nanostructures/Fe_3O_4@SiO_2/DABCO modified screen printed electrode for highly selective detection of epirubicin. *Biosensors and Bioelectronics* **91** (2017) 650-657. https://doi.org/10.1016/j.bios.2017.01.025

[2] S. Charak, D.K. Jangir, G. Tyagi, R. Mehrotra. Interaction studies of Epirubicin with DNA using spectroscopic techniques. *Journal of Molecular Structure*, **1000** (2011) 150-154. https://doi.org/10.1016/j.molstruc.2011.06.013

[3] R. Li, L. Dong, J. Huang. Ultra performance liquid chromatography-tandem mass spectrometry for the determination of epirubicin in human plasma. *Analytica Chimica Acta* **546** (2005) 167-173. https://doi.org/10.1016/j.aca.2005.04.073

[4] E.G. Mayhew, D. Lasic, S. Babbar, F.J. Martin. Pharmacokinetics and antitumor activity of epirubicin encapsulated in long-circulating liposomes incorporating a polyethylene glycol-derivatized phospholipid. *International Journal of Cancer* **51** (1992) 302-309. https://doi.org/10.1002/ijc.2910510221

[5] T. Liu, Y. Liao, H. Tao, J. Zeng, G. Wang, Z. Yang, Y. Wang, Y. Xiao, J. Zhou, X. Wang. RNA interference-mediated depletion of TRPM8 enhances the efficacy of epirubicin chemotherapy in prostate cancer LNCaP and PC3 cells. *Oncology Letters* **15** (2018) 4129-4136. https://doi.org/10.3892/ol.2018.7847

[6] A. Erdem, M. Ozsoz. Interaction of the anticancer drug epirubicin with DNA. *Analytica Chimica Acta* **437** (2001) 107-114. https://doi.org/10.1016/S0003-2670(01)00942-4

[7] H. Roché, P. Fumoleau,M. Spielmann, J.L. Canon, T. Delozier, D. Serin,M. Symann, P. Kerbrat, P. Soulié, F. Eichler. Sequential adjuvant epirubicin-based and docetaxel chemotherapy for node-positive breast

cancer patients: the FNCLCC PACS 01 Trial. *Journal of Clinical Oncology* **24** (2006) 5664-5671. https://doi.org/10.1200/JCO.2006.07.3916

[8] A.F. Okines, S.E. Ashley, D. Cunningham, J. Oates, A. Turner, J. Webb, C. Saffery, Y. Jo Chua, I. Chau. Epirubicin, oxaliplatin, and capecitabine with or without panitumumab for advanced esophagogastric cancer: dose-finding study for the prospective multicenter, randomized, phase II/III REAL-3 trial. *Journal of Clinical Oncology* **28** (2010) 3945-3950. https://doi.org/10.1200/JCO.2010.29.284

[9] M. Hasanzadeh, N. Shadjou. Pharmacogenomic study using bio-and nanobioelectrochemistry: drug-DNA interaction, *Materials Science and Engineering: C* **61** (2016) 1002-1017. https://doi.org/10.1016/j.msec.2015.12.020

[10] A. Khodadadi, E. Faghih-Mirzaei, H. Karimi-Maleh, A. Abbaspourrad, S. Agarwal, V.K. Gupta. A new epirubicin biosensor based on amplifying DNA interactions with polypyrrole and nitrogen-doped reduced graphene: experimental and docking theoretical investigations. *Sensors and Actuators B: Chemical* **284** (2019) 568-574. https://doi.org/10.1016/j.snb.2018.12.164

[11] S. Wang, Z. Huang, M. Liu, Y. Liu, H. Ding. Application of disposable screen-printed electrode as an epirubicin sensor and relation among whole blood and tissue concentrations of epirubicin. *International Journal of Electrochemical Science* **7** (2012) 1543-1555. https://doi.org/10.1016/S1452-3981(23)13434-1

[12] N. Treder, O. Maliszewska, I. Oledzka, P. Kowalski, N. Miekus, T. Baczek, E. Bien, M.A. Krawczyk, E. Adamkiewicz-Droiynska, A. Plenis. Development and validation of a high-performance liquid chromatographic method with a fluorescence detector for the analysis of epirubicin in human urine and plasma, and its application in drug monitoring. *Journal of Chromatography B* **1136** (2020) 121910. https://doi.org/10.1016/j.jchromb.2019.121910

[13] K.E. Maudens, C.P. Stove, V.F. Cocquyt, H. Denys, W.E. Lambert. Development and validation of a liquid chromatographic method for the simultaneous determination of four anthracyclines and their respective 13-S-dihydro metabolites in plasma and saliva. *Journal of Chromatography B* **877** (2009) 3907-3915. https://doi.org/10.1016/j.jchromb.2009.09.044

[14] P. Gopinath, S. Veluswami, R. Thangarajan, G. Gopisetty. RP-HPLC-UV method for estimation of fluorouracil-epirubicin-cyclophosphamide and their metabolite mixtures in human plasma (matrix). *Journal of Chromatographic Science* **56** (2018) 488-497. https://doi.org/10.1093/chromsci/bmy020

[15] G.R. Bardajee, M. Sharifi, M. Khanahmadi. An efficient method for detection of Epirubicin via Gelatin-CdTe/ZnS QDs as a nano-bioconjugated fluorescent sensor. *Physica B* **645** (2022) 414283. https://doi.org/10.1016/j.physb.2022.414283

[16] D.M. Souza, J.F. Reichert, A.F. Martins. A simultaneous determination of anti-cancer drugs in hospital effluent by DLLME HPLC-FLD, together with a risk assessment. *Chemosphere* **201** (2018) 178-188. https://doi.org/10.1016/j.chemosphere.2018.02.164

[17] N. Guichard, M. Ogereau, L. Falaschi, S. Rudaz, J. Schappler, P. Bonnabry, S. Fleury-Souverain. Determination of 16 antineoplastic drugs by capillary electrophoresis with UV detection: Applications in quality control. *Electrophoresis* **39** (2018) 2512-2520. https://doi.org/10.1002/elps.201800007

[18] G. Whitaker, A. Lillquist, S.A. Pasas, R. O'Connor, F. Regan, C.E. Lunte, M. R. Smyth. CE-LIF method for the separation of anthracyclines: application to protein binding analysis in plasma using ultrafiltration. *Journal of Separation Science* **31** (2008) 1828-1833. https://doi.org/10.1002/jssc.200700629

[19] I. Eman, A.F. El-Yazbi. An eco-friendly stability-indicating spectrofluorimetric method for the determination of two anticancer stereoisomer drugs in their pharmaceutical preparations following micellar enhancement: Application to kinetic degradation studies. *Spectrochimica Acta A* **163** (2016) 145-153. https://doi.org/10.1016/j.saa.2016.03.034

[20] J. Mo, L. Shen, Q. Xu, J. Zeng, J. Sha, T. Hu, K. Bi, Y. Chen. An Nd^{3+}-sensitized upconversion fluorescent sensor for epirubicin detection. *Nanomaterials* **9** (2019) 1700. https://doi.org/10.3390/nano9121700

[21] A.B. Hashkavayi, J.B. Raoof. Design an aptasensor based on structure-switching aptamer on dendritic gold nanostructures/Fe_3O_4@SiO_2/DABCO modified screen printed electrode for highly selective detection of epirubicin. *Biosensors and Bioelectronics* **91** (2017) 650-657. https://doi.org/10.1016/j.bios.2017.01.025

[22] H. Zhang. Fabrication of a single-walled carbon nanotube-modified glassy carbon electrode and its application in the electrochemical determination of epirubicin. *Journal of Nanoparticle Research* **6** (2004) 665-669. https://doi.org/10.1007/s11051-004-3723-7

[23] S. Tajik, H. Beitollahi, S. A. Ahmadi, M. B. Askari, A.Di Bartolomeo. Screen-printed electrode surface modification with $NiCo_2O_4$/RGO nanocomposite for hydroxylamine detection. *Nanomaterials* **11** (2021) 3208. https://doi.org/10.3390/nano11123208

[24] S. Tajik, H. Beitollahi, F. Garkani Nejad, Z. Dourandish. Electrochemical determination of doxorubicin in the presence of dacarbazine using MWCNTs/ZnO nanocomposite modified disposable screen-printed electrode. *Biosensors* **15** (2025) 60. https://doi.org/10.3390/bios15010060

[25] R.M. Silva, A.D. da Silva, J.R. Camargo, B.S. de Castro, L.M. Meireles, P.S. Silva, T.A. Silva. Carbon nanomaterials-based screen-printed electrodes for sensing applications. *Biosensors* **13** (2023) 453. https://doi.org/10.3390/bios13040453

[26] X. Liu, Y. Yao, Y. Ying, J. Ping. Recent advances in nanomaterial-enabled screen- printed electrochemical sensors for heavy metal detection. *Trends in Analytical Chemistry* **115** (2019) 187-202. https://doi.org/10.1016/j.trac.2019.03.021

[27] H. Beitollahi, J.B. Raoof, R. Hosseinzadeh. Electroanalysis and simultaneous determination of 6-thioguanine in the presence of uric acid and folic acid using a modified carbon nanotube paste electrode. *Analytical Sciences* **27** (2011) 991-991. https://doi.org/10.2116/analsci.27.991

[28] Z. Zhang, H. Karimi-Maleh. In situ synthesis of label-free electrochemical aptasensor-based sandwich-like AuNPs/PPy/$Ti_3C_2T_x$ for ultrasensitive detection of lead ions as hazardous pollutants in environmental fluids, *Chemosphere* **324** (2023) 138302. https://doi.org/10.1016/j.chemosphere.2023.138302

[29] H. Beitollahi, S. Ghofrani Ivari, M. Torkzadeh-Mahani. Voltammetric determination of 6-thioguanine and folic acid using a carbon paste electrode modified with ZnO-CuO nanoplates and modifier, *Materials Science and Engineering: C* **69** (2016) 128-133. https://doi.org/10.1016/j.msec.2016.06.064

[30] Z. Zhang, H. Karimi-Maleh. Label-free electrochemical aptasensor based on gold nanoparticles/titanium carbide MXene for lead detection with its reduction peak as index signal. *Advanced Composites and Hybrid Materials* **6** (2023) 68. https://doi.org/10.1007/s42114-023-00652-1

[31] S. Tajik, M.A. Taher, H. Beitollahi. First report for electrochemical determination of levodopa and cabergoline: application for determination of levodopa and cabergoline in human serum, urine and pharmaceutical formulations. *Electroanalysis* **26** (2014) 796-806. https://doi.org/10.1002/elan.201300589

[32] S. Tajik, M.A. Taher, H. Beitollahi. Simultaneous determination of droxidopa and carbidopa using a carbon nanotubes paste electrode. *Sensors and Actuators B: Chemical* **188** (2013) 923-930. https://doi.org/10.1016/j.snb.2013.07.085

[33] S. Zheng, N. Zhang, L. Li, T. Liu, Y. Zhang, J. Tang, S. Su. Synthesis of graphene oxide-coupled CoNi bimetallic MOF nanocomposites for the simultaneous analysis of catechol and hydroquinone. *Sensors* **23** (2023) 6957. https://doi.org/10.3390/s23156957

[34] H. Beitollahi, S. Tajik, F. Garkani Nejad. (Fe)-NH_2 meta-organic framework/graphene oxide nanocomposite modified screen-printed carbon electrode for electrochemical sensing of 2,4-dichlorophenol in water samples. *Heliyon* **11** (2025) e42285. https://doi.org/10.1016/j.heliyon.2025.e42285

[35] J. Mei, J. Han, F. Wu, Q. Pan, F. Zheng, J. Jiang, Q. Li. SnS@C nanoparticles anchored on graphene oxide as high-performance anode materials for lithium-ion batteries. *Frontiers in Chemistry* **10** (2023) 1105997. https://doi.org/10.3389/fchem.2022.1105997

[36] S. Tajik, H. Beitollahi, F. Garkani Nejad, R. Zaimbashi. $CoWO_4$/reduced graphene oxide nanocomposite-modified screen-printed carbon electrode for enhanced voltammetric determination of 2,4-dichlorophenol in water samples. *Micromachines* **15** (2024) 1360. https://doi.org/10.3390/mi15111360

[37] C. Bhuvaneswari, A. Elangovan, C. Sharmila, K. Sudha, G. Arivazhagan. Fabrication of cobalt tungstate/N-rGO nanocomposite: Application towards the detection of antibiotic drug-Furazolidone. *Colloids and Surfaces A: Physicochemical and Engineering Aspects* **656** (2023) 130299. https://doi.org/10.1016/j.colsurfa.2022.130299

[38] T. Nandagopal, G. Balaji, S. Vadivel. Tuning the morphology and size of $NiMoO_4$ nanoparticles anchored on reduced graphene oxide (rGO) nanosheets: The optimized hybrid electrodes for high energy density asymmetric supercapacitors. Journal of Electroanalytical Chemistry **928** (2023) 116944. https://doi.org/10.1016/j.jelechem.2022.116944

[39] L.W. Bai, Y.F. Shi, X. Zhang, X.B. Liu, F. Wu, C. Liu, W.B. Lu. A two-dimensional $NiMoO_4$ nanowire electrode for the sensitive determination of hydroquinone in four types of actual water samples. *Journal of Analysis and Testing* **6** (2022) 382-392. https://doi.org/10.1007/s41664-022-00236-w

[40] K.S. Ranjith, A.E. Vilian, S.M. Ghoreishian, R. Umapathi, S.K. Hwang, C.W. Oh, Y.K. Han. Hybridized 1D-2D $MnMoO_4$-MXene nanocomposites as high-performing electrochemical sensing platform for the sensitive detection of dihydroxybenzene isomers in wastewater samples. *Journal of Hazardous Materials* **421** (2022) 126775. https://doi.org/10.1016/j.jhazmat.2021.126775

[41] C. Ling, L. Zhou, H. Jia. First-principles study of crystalline $CoWO_4$ as oxygen evolution reaction catalyst. *RSC Advances* **4** (2014) 24692-24697. https://doi.org/10.1039/C4RA03893B

[42] H. Jia, J. Stark, L. Zhou, C. Ling, T. Sekito, Z. Markin. Different catalytic behavior of amorphous and crystalline cobalt tungstate for electrochemical water oxidation. *RSC Advances* **2** (2012) 10874-10881. https://doi.org/10.1039/C2RA21993J

[43] J. Zhang, J. Wei, J. Li, M. Xiahou, Z. Sun, A. Cao, Y. Chen. Delicate construction of Z-scheme heterojunction photocatalysts by ZnS quantum dots wrapped $CoWO_4$ nanoparticles for highly efficient environmental remediation. *ACS Applied Nano Materials* **7** (2024) 20101-20113. https://doi.org/10.3390/mi15111360

[44] B. Sriram, S. Gouthaman, S.F. Wang, Y.F. Hsu. Cobalt molybdate hollow spheres decorated graphitic carbon nitride sheets for electrochemical sensing of dimetridazole. *Food Chemistry* **430** (2024) 136853. https://doi.org/10.1016/j.foodchem.2023.136853

[45] Y. Li, J. Zheng, J. Yan, Y. Liu, M. Guo, Y. Zhang, C. Meng. La-doped $NiWO_4$ coupled with reduced graphene oxide for effective electrochemical determination of diphenylamine. *Dalton Transactions* **52** (2023) 12808-12818. https://doi.org/10.1039/D3DT02524A

[46] S. Ramanathan, A. Thamilselvan, N. Radhika, D. Padmanabhan, A. Durairaj, A. Obadiah, S. Vasanthkumar. Development of rutin-rGO/TiO_2 nanocomposite for electrochemical detection and photocatalytic removal of 2,4-DCP, *Journal of the Iranian Chemical Society* **18** (2021) 2457-2472. https://doi.org/10.1007/s13738-021-02205-z

[47] R. Kumar, T. Bhuvana, A. Sharma. Nickel tungstate-graphene nanocomposite for simultaneous electrochemical detection of heavy metal ions with application to complex aqueous media. *RSC Advances* **7** (2017) 42146-42158. https://doi.org/10.1039/C7RA08047F

[48] X. Xu, J. Shen, N. Li, M. Ye. Facile synthesis of reduced graphene oxide/$CoWO_4$ nanocomposites with enhanced electrochemical performances for supercapacitors. *Electrochimica Acta* **150** (2014) 23-34. https://doi.org/10.1016/j.electacta.2014.10.139